

Neutron transition multipole moment for $^{88}\text{Sr}(\alpha, \alpha')^{88}\text{Sr}^*(2^+, 1.84 \text{ MeV})$

S. K. Datta, Subinit Ray, H. Majumdar, S. K. Ghosh, and C. Samanta
Saha Institute of Nuclear Physics, I/AF, Bidhan Nagar, Calcutta 700 064, India

S. Ray and P. Dasgupta
Department of Physics, Kalyani University, Kalyani, West Bengal 741 235, India

S. N. Chintalapudi and S. R. Banerjee
Variable Energy Cyclotron Centre, Bhabha Atomic Research Centre, I/AF, Bidhan Nagar, Calcutta 700 064, India
(Received 20 September 1988)

The neutron transition multipole moment, M_n , for ($0^+ \rightarrow 2^+$, 1.84 MeV) transition is inferred by measuring the (α, α') angular distribution at $E_\alpha = 50$ MeV and comparing it with a microscopic distorted-wave Born approximation calculation. Proton transition densities are taken from electron scattering data. M_n/M_p is found to be substantially less than N/Z in agreement with the (p, p') result.

The advent of precision high-energy electron scattering techniques leading to detailed information of the proton transition densities ρ_p , has ushered in a new era of knowledge in nuclear structure studies.¹ Similar information on the neutron transition densities ρ_n , is not easily available. The neutron transition multipole moment M_n , involving the volume integral of ρ_n , however, can be inferred from a study of (α, α') angular distributions and comparing the experimental data with the microscopic distorted-wave-Born approximation (DWBA) calculation.²⁻⁵ The DWBA calculation includes both ρ_p and ρ_n , and if ρ_p is known from electronic scattering, indirect information on ρ_n , or at least M_n , may be obtained.

This method has been employed by Kobos *et al.*,⁶ to obtain M_n/M_p for $^{90}\text{Zr}(\alpha, \alpha')^{90}\text{Zr}^*(2^+, 2.186 \text{ MeV})$, among other things. The value of M_n/M_p found was 0.63. Recently, Rychel *et al.*,⁷ using a Coulomb-nuclear interference technique, found the same M_n/M_p to be 1.22 ± 0.12 . Now, Bernstein *et al.*⁸⁻¹⁰ have shown that M_n/M_p should be less than the pure collective model value, N/Z (1.25 for ^{90}Zr) for single closed-shell proton valence nuclei. While the Kobos result agrees with Bernstein's calculations, Rychal's measurement seems to reproduce the pure collective model value.

Now, ^{88}Sr is very similar in configuration to ^{90}Zr . Having only two protons less, it is definitely a single closed-shell ($N=50$) proton valence nucleus. Recently, Kouw *et al.*^{11,12} have explained the $^{88}\text{Sr}(p, p')^{88}\text{Sr}^*(2^+, 1.84 \text{ MeV})$ angular distributions quite satisfactorily by a microscopic DWBA calculation with ρ_p and ρ_n calculated from a broken-pair model. The neutron transition densities,¹¹ while having the same shape as ρ_p , are smaller than the latter by about 20–30% in magnitude, indicating $M_n/M_p < 1$. The ratio of the deformation lengths for neutron and proton $\delta(n)/\delta(p)$ which could be related to M_n/M_p (Ref. 2), is found to be 0.61 ± 0.16 . This is less than $N/Z=1.3$, lending support to Bernstein's calculations. What is the result from (α, α') studies?

So far, there are only two investigations in the $^{88}\text{Sr}(\alpha, \alpha')^{88}\text{Sr}^*$ at 42 MeV (Ref. 13) and at 166 MeV.¹⁴ The earlier work did not extract M_p or M_n ; although Bernstein *et al.*^{2,8} used these data to report a value of M_n/M_p for $^{88}\text{Sr}(2^+, 1.84 \text{ MeV} \text{ state})$. This value is less than N/Z , but the associated error is 30% or more. The later work, at 166 MeV, included a microscopic analysis with transition densities calculated from 1p-1h RPA random-phase approximation, but the agreement with the data was very poor.¹⁴ They concluded this to be due to the neglect of 2p-2h contributions, an inference supported in later RPA calculations¹⁵ for $^{88}\text{Sr}(e, e')^{88}\text{Sr}^*$.

There was thus scope for obtaining new information on M_n for the ($0^+ \rightarrow 2^+$, 1.84 MeV) transition in ^{88}Sr by (α, α') reaction studies, provided it was done reasonably accurately, taking into account newer developments in theory such as density dependent forms of effective interaction. We planned the experiment at 50 MeV, a suitable energy for our machine, and confined our measurements to forward angles from $\sim 6^\circ$ to 82° , where one can hope that a direct reaction description is applicable.

The experiment was carried out with an unanalyzed beam from the variable energy cyclotron, Calcutta. The target was prepared by reducing natural Sr (NO_3)₂ with Al powder and then evaporating it onto a $20 \mu\text{g}/\text{cm}^2$ carbon backing. The target thickness was $350 \mu\text{g}/\text{cm}^2$. Si-Li detectors of 2 mm active thickness were used. Particle identification was not necessary, since competing reaction channels (α, d) , (α, t) , and $(\alpha, ^3\text{He})$ have high negative Q values. Energy loss of 50 MeV protons in the 2 mm detector is also too small to cause any interference in the region of interest. Conventional electronics was used and data acquisition was effected through a S-88 Canberra multichannel analyzer. A typical spectrum for the region of interest at $\Theta=45^\circ$ is shown in Fig. 1. The energy resolution was about 250 keV. A monitor detector was put at $\Theta=40^\circ$ and absolute normalization of the data was obtained by comparing the elastic cross section at this angle

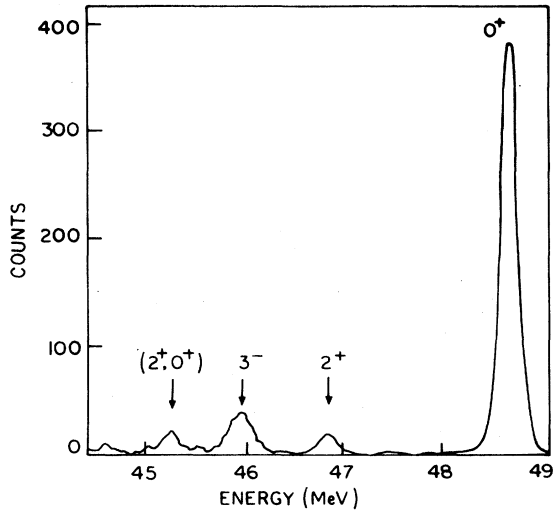


FIG. 1. Energy spectrum of $^{88}\text{Sr}(\alpha, \alpha')^{88}\text{Sr}^*$ reaction at $E_\alpha = 50$ MeV and $\Theta = 45^\circ$.

to an optical model fit. The error in the absolute cross section is approximately 20%.

The differential cross sections for α elastic scattering from ^{88}Sr , for angles ranging from 10° to 82° , are shown in Fig. 2. Error bars include only statistical uncertainties. It was not possible to take elastic data forward of 10° because of interference from oxygen and carbon impurities. The solid line shown is a best-fit optical model calculation with conventional parametrization

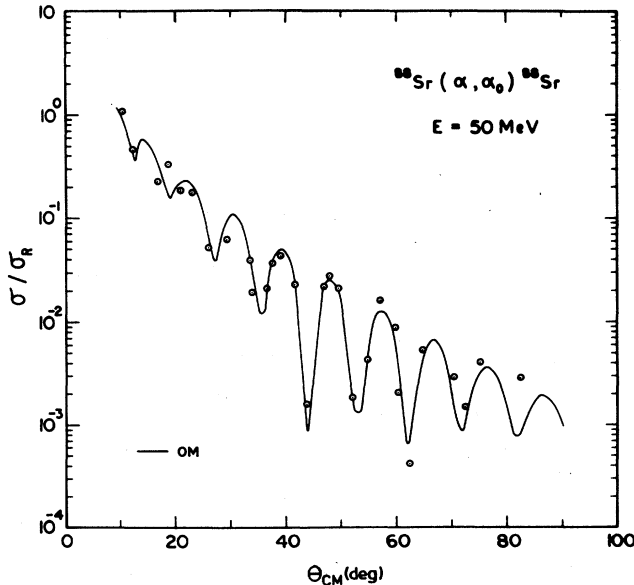


FIG. 2. Elastic angular distribution (ratio to Rutherford) for α scattering on ^{88}Sr . The solid line is an optical model calculation with parameters from Table I.

$$V(r) = \frac{-v_0}{1 + e^{(r-R_0)/a_0}} + \frac{-iW_s}{1 + e^{(r-R_w)/a_w}} + \frac{-4iW_a e^{(r-R_w)/a_w}}{[1 + e^{(r-R_w)/a_w}]^2} + V_{\text{Coul}}(r). \quad (1)$$

The parameters used are reported in Table I. Woods-Saxon potentials raised to some power n , was also used as suggested by Gubler *et al.*,¹⁶ but this did not improve the quality of the fit. We did not try to perform a microscopic folding model calculation for the elastic data as in Refs. 6 and 14, as we feel that it is well established that microscopic calculations fit α -elastic data very well. But for our purpose, where we concentrate on the off-diagonal parts of interaction, the phenomenological optical model would serve just as well.

The data for inelastic scattering to the first excited 1.84 MeV, 2^+ state in the angular range 6° – 82° are shown in Fig. 3. No data could be extracted in the 22° – 26° range due to interference from oxygen and carbon impurities. The solid line is a DWBA calculation with a collective model form factor, using the computer code DWUCK4 of Kunz.¹⁷ Optical model parameters of Table I were used. The vibrational parameter β_2 obtained from the fit was 0.065. It is observed that the DWBA calculation reproduces the general trend of the data although the fit in the larger angles is rather poor. The same disagreement was observed in the earlier works of Alster *et al.*¹³ and Bimbot *et al.*¹⁴ A coupled-channels calculation was also performed with $0^+ - 2_1^+ - 2_2^+$ coupling in the vibrational model, assuming one and two phonon states, by using the code JUPITOR of Tamura.¹⁸ $\beta_2 = 0.065$ was used for the coupling between the ground state and the first 2^+ state. The resulting calculation was practically identical to the DWBA output and is not shown.

The microscopic calculation for the inelastic scattering was carried out using the deformed folding model.^{6,19} The real part of the radial form factor for the l th multipole may be written as²

$$F_l(r_\alpha) = \int \rho(r) V_l(r, r_\alpha) r^2 dr, \quad (2)$$

where $V_l(r, r_\alpha)$ is related to α - N effective interaction by

$$V_{\alpha N}(\bar{r}, \bar{r}_\alpha) = \sum_{l,m} V_l(r, r_\alpha) Y_{lm}^*(r_\alpha) Y_{lm}(r), \quad (3)$$

and $\rho(r)$ is the transition density from ground state $|0^+\rangle$ to the excited state $|2^+\rangle$

$$\rho(r) = \langle 2^+ || \sum_j Y_2(r_j) || 0^+ \rangle. \quad (4)$$

Actually, one defines separately ρ_p and ρ_n , so that

$$\rho(r) = \rho_p(r) + \rho_n(r), \quad (5)$$

the sum over j in Eq. (4), running over either protons or neutrons. The proton and neutron transition multipole moments (for $0^+ \rightarrow 2^+$) are defined as

$$M_i = \int \rho_i(r) r^4 dr, \quad (6)$$

TABLE I. Optical model parameters.

Channel	V_0 (MeV)	R_0 (fm)	a_0 (fm)	W_s (MeV)	W_d (MeV)	R_w (fm)	a_w (fm)	R_C (fm)
$\alpha + {}^{88}\text{Sr}$	54.51	1.45	0.72	21.96	5.86	1.43	0.63	1.25

where i stands for p or n . The electromagnetic transition rate $B(E2)$ is related to M_p by

$$B(E2, I_i - I_f) = \frac{e^2 |M_p|^2}{2I_i + 1} = e^2 |M_p|^2 \quad (7)$$

for the 0^+ ground state.

In our analysis, we took the proton transition charge density $\rho_p(r)$ for ${}^{88}\text{Sr}(2^+, 1.84 \text{ MeV})$ from electron scattering data of Schwentker *et al.*²⁰ We then obtained the normalization of ρ_p by calculating $|M_p|^2$ from (6) and equating it to

$$B(E2) = 925 e^2 \text{ fm}^4$$

from the work of Raman *et al.*²¹ This normalization is $2.2 \approx \sqrt{5}$, due to an extra factor of $\sqrt{2I+1}$ between the two definitions of Ref. 20 and 21.

As for the neutron transition density ρ_n , its shape was assumed to be the same as that of ρ_p , an assumption consistent with the broken-pair model calculation of Kouw *et al.*¹¹ To determine the magnitude of ρ_n we used an ar-

bitrary normalization factor N so that $\rho_n = N\rho_p$. Putting this in Eq. (2), we can write the real part of the form factor as

$$F_l(r) = (1+N) \int \rho_p(r) V_l(r, r_\alpha) r^2 dr. \quad (8)$$

Since the normalized ρ_p is completely known, as discussed before, we only have to use a proper effective interaction, $V_l(r, r_\alpha)$, in the preceding equation to get $F_l(r)$. N would be determined by fitting the experimental cross section.

The effective interactions, $V_{\alpha N}$, that we have used are (i) single folding Gaussian interaction,²

$$V_{\alpha N} = -V_0 \exp(-\gamma \times |r - r_\alpha|^2)$$

with $V_0 = 37 \text{ MeV}$ and $\gamma = 0.25 \text{ fm}^{-2}$ (ii) Gaussian interaction with a dynamic density dependence^{19,22}

$$V_{\alpha N} = -64.6 \exp\left(\frac{-|r - r_\alpha|^2}{a^2}\right) \times \left(1 - \frac{5}{3} \gamma \rho^{2/3}\right)$$

with $a = 1.798 \text{ fm}$, $\gamma = 1.9 \text{ fm}^2$, and the ground-state density ρ for ${}^{88}\text{Sr}$ taken from electron scattering data of DeVries *et al.*²³ and assuming the same density for protons and neutrons (iii) superposition of a Gaussian Yukawa with a density dependence²⁴

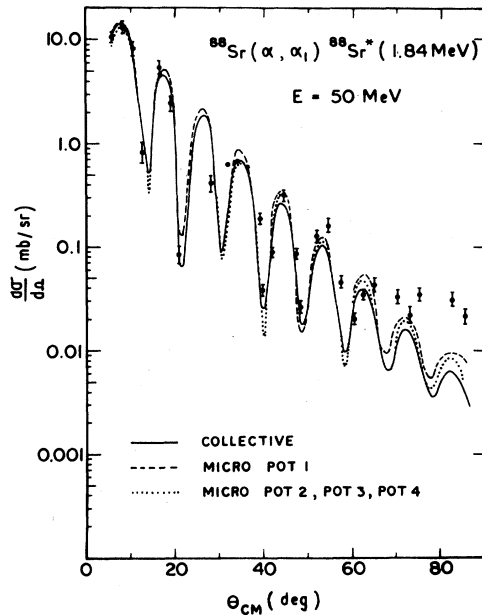


FIG. 3. Differential cross section for ${}^{88}\text{Sr}(\alpha, \alpha'){}^{88}\text{Sr}^*(2^+, 1.84 \text{ MeV})$ reaction. The solid line is a DWBA calculation with collective model form factor and the dashed, dotted lines are those with microscopic form factors, calculated with density-independent Gaussian (POT 1), density-dependent Gaussian (POT 2), superposition of Gaussian and Yukawa (POT 3), and density-independent Hasegawa (POT 4).

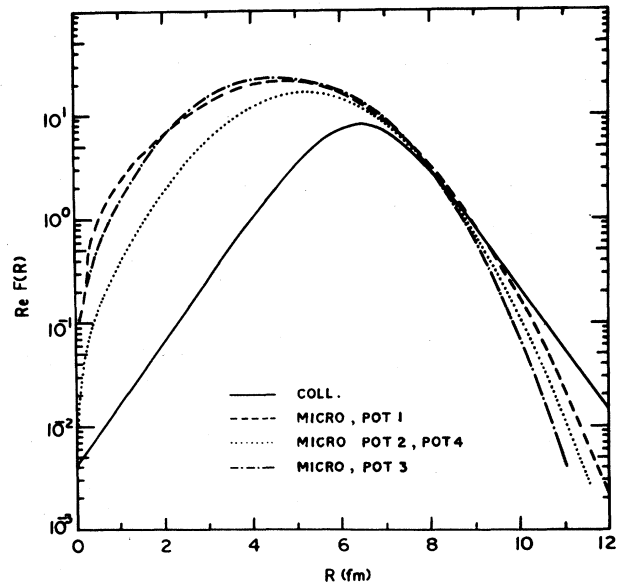


FIG. 4. Real part of radial form factor $F(R)$ as a function of R . The solid line is for the collective model and the dashed, dotted, dashed-dotted lines are microscopic calculations for different effective interactions.

TABLE II. M_n/M_p values.

Pot 1 Gaussian density independent	Pot 2 Gaussian density dependent	Pot 3 Gaussian + Yukawa density dependent	Pot 4 Hasegawa density independent
0.64	0.85	0.85	0.85

$$V_{\alpha N} = \left\{ -64.6 \exp \left[-\frac{|r-r_\alpha|^2}{(1.798)^2} \right] - 77.0 \frac{\exp(-\mu|r-r_\alpha|)}{\mu|r-r_\alpha|} \right\} \left(1 - \frac{5}{3} \gamma \rho^{2/3} \right),$$

with $\mu = 1.176 \text{ fm}^{-1}$ and (iv) double folded Hasegawa interaction,²⁵ where the basic nucleon-nucleon interaction

$$V_{nn} = 616 \exp(-r/0.542)^2 - 195 \exp(-r/0.942)^2$$

is folded over the α -particle ground-state density,²⁶

$$\rho_\alpha(r) = 0.4229 \exp(-0.7024r^2),$$

to obtain an αN potential. The purpose of using all these different interactions was to determine if the calculated cross section was reasonably model independent so as to attach some confidence to our extracted value of M_n/M_p . The real part of the form factor calculated with different $V_{\alpha N}$ and appropriate N values to fit the data are shown in Fig. 4. The important thing is that $F_l(r)$ values are almost identical for various models in the range of $r = 6-9$ fm. For larger values of r , $F_l(r)$ is too small; for smaller r values, attenuation of distorted waves produces very little contribution.

For the imaginary part of the radial form factor, the collective model imaginary form factor $\beta_I r_W dW/dr$ was used, W including both the volume and the surface imaginary terms. The radius of the imaginary potential, $r_W = R_W A^{1/3}$, with R_W from Table I, and $\beta_I = 0.065$ from the collective model fit. This β_I is very similar to that obtained for ^{90}Zr by the detailed procedure of Kobos *et al.*,⁶ equating the deformation parameters for charge distribution and imaginary potential.

The form factors thus generated were used in DWUCK4 to obtain the microscopic inelastic calculation shown by various lines in Fig. 3. The normalization constant N in $F_l(r)$, adjusted to fit the magnitude of experimental $d\sigma/d\Omega$ in the forward peak, is equal to M_n/M_p from Eq. (6), since in our assumption, $\rho_n = N\rho_p$. The various values of M_n/M_p for different models are shown in Table II. For the different interactions, we obtain almost the same value of $M_n/M_p \sim 0.85$. The density independent Gaussian interaction gives a somewhat different value of 0.64. These values are comparable with $\delta(n)/\delta(p)$ of Kouw *et al.*¹² (which reduces to M_n/M_p , in our method of derivation) 0.61 ± 0.16 . Differences in the magnitude of cross section (of the order of 30%–40%) between density dependent and density independent interaction calculations have also been observed by El Ahrab *et al.*²⁷ In any case, the absolute error in our cross-section data is estimated to be about 20%. The model dependence in our determination of M_n is comparable to this value. Our value of M_n/M_p is also consistent with Bernstein's calculations.¹⁰

We thank Dr. D. K. Srivastava for many helpful discussions and the cyclotron staff for operation of the machine. Assistance of detector and target laboratory personnel of The Variable Energy Cyclotron Centre (VECC) is gratefully acknowledged.

¹B. Frois, in *Proceedings of the International Conference on Nuclear Physics, Florence, 1983*, edited by P. Blassi and R. A. Ricci (Tipografia Compositori, Bologna, 1983), Vol. 2, p. 221.

²A. M. Bernstein, in *Advances in Nuclear Physics*, edited by M. Baranger and E. Vogt (Plenum, New York, 1969), Vol. 3, p. 325.

³H. Rebel, *Z. Phys. A* **277**, 35 (1976).

⁴A. M. Bernstein, R. A. Miskimen, B. Quinn, S. A. Wood, M. V. Hynes, G. S. Blanpied, B. G. Ritchie, and V. R. Brown, *Phys. Rev. Lett.* **49**, 451 (1982).

⁵A. Saha, K. K. Seth, M. Artuso, B. Harris, R. Seth, H. Nann, and W. W. Jacobs, *Phys. Rev. Lett.* **52**, 1876 (1984).

⁶A. M. Kobos, B. A. Brown, R. Lindsay, and G. R. Satchler, *Nucl. Phys. A* **425**, 205 (1984).

⁷D. Rychel, R. Gyufko, B. van Kruchten, M. Lahanas, P. Singh, and C. A. Wiedner, *Z. Phys. A* **326**, 455 (1987).

⁸A. M. Bernstein, V. R. Brown, and V. A. Madsen, *Phys. Lett.*

71B, 48 (1977).

⁹A. M. Bernstein, V. R. Brown, and V. A. Madsen, *Phys. Lett.* **103B**, 255 (1981).

¹⁰A. M. Bernstein, V. R. Brown, and V. A. Madsen, *Comments Nucl. Part. Phys.* **11**, 203 (1983).

¹¹L. R. Kouw, H. P. Blok, M. Pignanelli, R. De Leo, and M. N. Harakeh, *Phys. Lett. B* **174**, 137 (1986).

¹²L. R. Kouw, H. P. Blok, and J. Blok, *Nucl. Phys. A* **488**, 13 (1988).

¹³J. Alster, D. C. Shreve, and R. J. Peterson, *Phys. Rev.* **144**, 999 (1966).

¹⁴L. Bimbot, B. Tatischeff, I. Brissaud, Y. Le Bornec, N. Frascaria, and A. Willis, *Nucl. Phys. A* **210**, 397 (1973).

¹⁵C. Conci, G. Co, and J. Speth, in *Annual Report 1984, Kernforschungsanlage Julich GmbH, Institut für Kernphysik*, edited by F. Grummer, O. Schult, H. Seyfarth, J. Speth and P. Turek, p. 218.

- ¹⁶H. P. Gubler, U. Kiebele, H. O. Meyer, G. R. Plattner, and I. Sick, Nucl. Phys. **A351**, 29 (1981).
- ¹⁷P. D. Kunz, Computer Code DWUCK4 (unpublished).
- ¹⁸T. Tamura, Computer Code JUPITOR (unpublished).
- ¹⁹R. Pesl, H. J. Gils, H. Rebel, E. Friedman, J. Buschmann, H. Klewe-Nebenius, and S. Zagromski, Z. Phys. A **313**, 111 (1983).
- ²⁰O. Schwentker, J. Dawson, J. Robb, J. Heisenberg, J. Lichtenstadt, C. N. Papanicolas, J. Wise, J. S. McCarthy, L. T. Vander Bijl, and H. P. Blok, Phys. Rev. Lett. **50**, 15 (1983).
- ²¹S. Raman, C. H. Malarkey, W. T. Milner, C. W. Nestor, and P. H. Stelson, At. Data Nucl. Data Tables **36**, 1 (1987).
- ²²D. K. Srivastava and H. Rebel, Z. Phys. A **316**, 225 (1984); J. Phys. G **10**, L127 (1984).
- ²³H. DeVries, C. W. De Jager, and C. De Vries, At. Data Nucl. Data Tables **36**, 495 (1987).
- ²⁴E. Friedman, H. J. Gils, and H. Rebel, Phys. Rev. C **25**, 1551 (1982).
- ²⁵M. Kamimura, Nucl. Phys. **A351**, 456 (1981).
- ²⁶G. R. Satchler and W. G. Love, Phys. Rep. **55**, 183 (1979).
- ²⁷M. El-Azab Farid and G. R. Satchler, Nucl. Phys. **A481**, 542 (1988).